American Journal of Condensed Matter Physics 2017, 7(3): 57-66
DOI: 10.5923/j.ajcmp.20170703.01

Thermodynamic and Surface Properties of Cr-X, (X = Mo, Fe) Liquid Alloys

Y. A. Odusote*, A. I. Popoola

Department of Physics, The Federal University of Technology, Akure, Nigeria

Abstract Thermodynamic and surface properties of Cr-Mo and Cr-Fe liquid alloys were studied using a simple scheme based on the formation of self-associates in conjunction with a statistical model founded on the concept of the layered structure near the interface. The phase-segregation tendencies in these liquid alloys were analyzed through the study of surface properties (surface tension and surface composition), transport properties (diffusion and viscosity) and microscopic functions (concentration fluctuations in the long-wavelength limit, $S_{cc}(0)$ and chemical short-range order parameter, α_1). The positive deviation of the properties of mixing of the two liquid alloys from ideality has been discussed. Results show that the degree of phase-separation in Cr-Fe, as gauged by the $S_{cc}(0)$ and α_1, is less than in Cr-Mo. The theoretical analysis reveals that the rate at which Cr-atoms segregate at the surface is higher in Cr-Fe, than in Cr-Mo alloys for all bulk concentrations.

Keywords Modelling, Segregation, Cr-Mo, Cr-Fe, Thermophysical properties

1. Introduction

Metal alloys in general offer some benefits over convention metals due to their increased mechanical strength, heat and chemical resistance, and reduced production costs. From technological viewpoints, binary and ternary alloy systems containing chromium such as Cr-Mo, Cr-Fe, Cr-Al, Cr-Mo-Al, Cr-Nb-Re and Cr-Fe-Mo-C etc., represent a class of alloy systems with excellent high-temperature strength, high ductility, good corrosion and oxidation resistance. These properties make them sought after in a wide range of applications from steel production and Ni-based super alloys to surgical implants [1, 2], including aerospace and automobile industries [3], structural materials for nuclear power plants [1, 4], complex bulk metallic glasses [5], heat-resistant and corrosion-resistant protective coatings [2, 6].

In order to enhance the tribological, structural and mechanical properties of chromium-based alloys to suit diverse service conditions, alloying with other elements such as molybdenum (Mo) has shown to be effective in improving the toughness and tribological properties of Cr-N coatings [7-11]. On the other hand, the ability of Mo to form Magnli phase oxides can be used to prepare materials with solid lubricant potential, which considerably reduce the coefficient of friction [12, 13].

* Corresponding author:
yisau24@yahoo.co.uk (Y. A. Odusote)
Published online at http://journal.sapub.org/ajcmp

The present work is motivated by the controversial and divergent results in literature concerning chromium-based alloys. For instance, thermodynamic measurement performed on solid Cr-Mo alloys in the temperature range of 1471 - 1773 K [14-17] showed that the data of Dickson et al. [17] are at variance with those of others. While negative deviations from ideality was reported for components activity coefficients of Cr-Mo alloys at 1673 K using the Knudsen effusion technique by Dickson et al. [17]. The measured activity of Cr in solid Cr-Mo alloys at 1873 K by Jacob and Kumar [14], the results of Laffitte and Kubaschewskil [15], and that of Kubaschewski and Chart [16] on the other hand, indicated positive deviations from ideality. Similarly, Cr-Fe has been studied widely both experimentally and theoretically by many authors [1, 18-27]. However, a recent review by Xiong et al. [26, 27] indicated that the commonly accepted result due to Andersson and Sundman [23] requires further thermodynamic reassessment in many aspects, among which is precise locations of the corresponding phase boundaries of the solidus and liquidus lines on its phase diagram [1].

At low temperatures, Cr-Mo and Cr-Fe alloys are endowed with miscibility gap of the body centered cubic (bcc) in the solid phase. Alloys within the miscibility gap tend to separate or decompose into a Cr-rich bcc phase (α'), Mo-rich bcc phase (α) and/or an Fe-rich bcc phase (α) [27, 28]. This phenomenon of phase separation in Cr-based alloys, known generally as the "475^o embrittlement" has resulted in increased hardness and reduced ductility in these alloys with aging [20, 28, 29]. Also, Quintela et al. [30]

recently observed that even a very small addition of only ≈ 1% of Mo or W to Cr-based coating alloys, lead to a spontaneous phase segregation. Consequently, attempts are being made by researchers to combine all available experimental information to achieve a consistent description of the phase equilibria and thermodynamics of the phases involved in Cr-Mo and Cr-Fe alloy systems [27, 31, 32].

The amount of research on Cr-based (both binary and higher order alloys in recent times, has being on steady increase due to its various industrial applications and the use of atomistic approaches in investigating their structural behaviour [1, 27, 28]. However, measurement of thermodynamic and thermophysical quantities of alloy systems containing elements such as Cr, which is a strongly electropositive metal like Mg, and often acts as a strong reducing agent are difficult. In particular, concerning the data of transport and surface properties of ternary Cr-based and its binary alloys, only the surface tension data of their pure components have been well documented [33]. Since, a systematic measure of both thermodynamic and thermophysical data over the whole range of composition and temperature can be almost impossible to perform. It is therefore expected that most of the missing thermodynamic value on binary and multi-component systems will come within theoretical framework, rather than from direct experiment.

For the design and development of reliable materials for high-temperature applications, the knowledge of thermodynamic and thermophysical quantities of these alloys is important in gaining qualitative insight into their mixing behaviour as well as aid in elucidating the energetics and structure at atomistic level in the melts and how they are coupled. The nature of the atomic interactions and structural re-adjustment of the constituent atoms in liquid Cr-Mo and Cr-Fe alloys can be gauged from the values of Hume-Rothery empirical factors such as electronegativity difference (E_{Cr}-E_{Mo} = -0.20, and E_{Cr}-E_{Fe} = -0.20) [34], the size ratio, V_{Mo}/V_{Cr} ≈ 1.30 and V_{Fe}/V_{Cr} ≈ 0.98 [35], and valency difference (=0 or =2) [35], respectively. Obviously, these factors can only provide partial information and are not sufficient to completely characterize the mixing behaviour in these alloys.

In the present study, a simple scheme developed by Singh and Sommer [36] for studying liquid alloy systems with miscibility gap tendencies has been utilized to model liquid Cr-Mo and Cr-Fe alloys at 1471 K and 1600 K, respectively. We intend to explain the energetic effects on these systems in terms of the interaction energy parameter W, that reproduces as closely as possible their various concentration dependent properties with a view to understand alloying nature of ordering or segregation tendencies in the molten alloys. Afterwards, the transport properties (diffusion and viscosity), microscopic functions (concentration-concentration fluctuations in the long-wavelength limits, $S_{cc}(0)$ and chemical short-range order parameter, α_1) and surface properties (surface concentration and surface tension) were studied from a theoretical viewpoint with the aim of correlating the properties of the liquid alloys in the bulk and at the surface.

Both Cr-Mo and Cr-Fe liquid alloys exhibited positive deviations from ideal mixture behaviour with positive energy parameters, W at the respective temperatures. The positive signs of energy parameters for Cr-Mo and Cr-Fe alloys imply repulsive interactions between constituents of the alloys, and further indicate that there is a general tendency for homo-coordination of atoms in both liquid alloy systems [36].

The theoretical formulations of the model based on the formation of self-associates in binary liquid alloys as related to the various thermodynamic quantities, microscopic functions, transport and surface properties are presented in the next section. This is followed by results and discussion in section 3, and conclusion in the last section.

2. Theoretical Formulation

Let a liquid binary alloy consists of $N_A = Nc_A$ atoms of element A and $N_B = Nc_B$ atoms of element B located at equivalent lattice sites, where the total number of atoms $N = N_A + N_B$ and form of a polyatomic matrix, leading to the formation of like-atom cluster or self-associates of the type A_μ and B_ν, i.e

$$\mu A \leftrightharpoons A_\mu \quad ; \quad \nu B \leftrightharpoons B_\nu \tag{1}$$

μ and ν are the numbers of atoms in the cluster of A_i and B_j type, and c_i, (i = A, B) being the mole fraction of components A and B in the alloy, respectively.

2.1. Thermodynamic and Microscopic Functions for the Bulk

Based on the assumption of self-associates, the standard expression for the Gibbs free energy of mixing, G_M for demixing liquid binary alloys which is dependent on the number of self-associates, n = μ/ν can be expressed as [36]:

$$\frac{G_M}{RT} = \left\{c_A \ln c_A + (1-c_A)\ln(1-c_A) + c_A \ln(1-\beta) + \ln\xi\right\} + c_A(1-c_A)\xi W \tag{2}$$

with

$$\xi = \frac{1}{1-\beta c_A} \quad , \quad \beta = 1 - \frac{1}{n} \quad , \quad W = \Omega_A\left(\frac{\omega}{k_B T}\right) \tag{3}$$

and

$$\omega = z\left(\epsilon_{AB} - (\epsilon_{AA} + \epsilon_{BB})/2\right) \tag{4}$$

The coordination number of the liquid alloys z is taken as 10 [37-39]. ϵ_{ij} are the energies of i–j pairs of atoms and ω defined by Eq. (4) is known as the interchange energy whose value gives insight into the nature of alloying in binary liquid alloys. Clearly, for a liquid alloy if ω < 0, there is tendency to form unlike atom pairs and if it is greater than zero, like atoms tend to pair together as nearest-neighbors. ω = 0, indicates that atoms in the mixture are perfectly disordered [38].

The concentration-concentration fluctuations at the long wavelength limits, $S_{cc}(0)$ can be readily obtained using standard thermodynamic relation in terms of the free energy of mixing as [36-39]:

$$S_{cc}(0) = RT\left(\frac{\partial^2 G_M}{\partial c_A^2}\right)^{-1}_{T,P,N} \quad (5)$$

Using Eqns. (2) and (5), an expression for $S_{cc}(0)$ is given by:

$$\frac{S_{cc}(0)}{S_{cc}^{id}(0)} = \left(1 - c_A(1-c_A)g(n,W)\right)^{-1} \quad (6)$$

where

$$g(n,W) = \frac{2n^2\left(\frac{W}{RT}\right) - (n-1)^2[(c_A + n(1-c_A)]}{[(c_A + n(1-c_A)]^3} \quad (7)$$

for ideal mixing, the energy parameter ω in Eq.(4) equal to zero, and Eq.(6) reduces to

$$S_{cc}^{id}(0) = c_A(1-c_A) \quad (8)$$

In the present approach, n and W are independent of concentration but may depend on pressure and temperature. The parameters (n, W) are the model parameters to be fitted at a given temperature to calculate the thermodynamic, transport and by extension the structural properties of the binary liquid alloys.

The Warren-Cowley chemical short range order parameter, (α_1), [40, 41] has been used to quantify the degree of order and segregation in the liquid alloys. This parameter α_1 is computed theoretically [36-38] via the relation:

$$\frac{S_{cc}(0)}{c(1-c)} = \frac{1+\alpha_1}{1+(z-1)\alpha_1} \quad (9)$$

In similar fashion with the aid of Eq. (2), expressions can be obtained for other thermodynamic quantities via standard thermodynamic relations:

$$RT\ln a_i = \left(\frac{\partial G_M}{\partial N_i}\right)_{T,P,N} \quad (10)$$

solving Eq. (10) and recall that $N = N_A + N_B$ with $c_A = N_A/N$, one obtains expressions for the component activities as:

$$\ln a_A = \ln[c_A\xi(1-\beta)] + (1-c_A)\xi\beta + (1-c_A)^2\xi^2\frac{W}{RT} \quad (11)$$

and

$$\ln a_B = \ln(c_A\xi) + c_A(1-\beta)\xi(1-n) + nc_A^2(1-\beta)\xi^2\frac{W}{RT} \quad (12)$$

The enthalpy of mixing H_M is given as:

$$H_M = G_M + TS_M \quad (13)$$

and the entropy of mixing, S_M is defined in terms of G_M as:

$$S_M = -\left(\frac{\partial G_M}{\partial T}\right)_P \quad (14)$$

putting Eq. (2) in Eq. (14), the entropy of mixing becomes:

$$S_M = -R\left[c_A\ln c_A + (1-c_A)\ln(1-c_A) + c_A\ln(1-\beta) + \xi\right] + c_A(1-c_A)\xi\frac{\partial W}{\partial T} \quad (15)$$

Segregating alloy systems are endowed with positive values of H_M.

2.2. Transport Properties: Diffusion and Viscosity

2.2.1. Diffusion

The formalism that relates diffusion and $S_{cc}(0)$ combines Darken's thermodynamic equation for diffusion with basic thermodynamic equation in the form [36, 39]:

$$\frac{D_M}{D_{id}} = \frac{S_{cc}^{id}(0)}{S_{cc}(0)} \quad (16)$$

where D_M is the mutual diffusion coefficient and D_{id} is the intrinsic diffusion coefficient for an ideal mixture. An understanding of Eq. (16) shows that $D_M/D_{id} < 1$ and $D_M/D_{id} > 1$ are signatures of homocoordination and heterocoordination, respectively. In addition, if $D_M/D_{id} \rightarrow 1$, it implies ideal mixing [37].

2.2.2. Viscosity

Taking into account the Strokes-Einstein type relation for liquid alloys, the viscosity, η is related to the $S_{cc}(0)$ and D_M (Eq.(16), by [42-43]:

$$\eta = \eta_o\phi \quad (17)$$

with the quantities ϕ and η_o defined as:

$$\phi = \frac{c_A c_B}{S_{cc}(0)} \quad ; \quad \eta_o = \frac{k_B T}{D_M}\left(\frac{c_A}{m_2} + \frac{c_B}{m_1}\right) \quad (18)$$

m_1 and m_2 are functions of the size and shape of the constituent particles; k_B is the Boltzmann's constant and T is the absolute temperature.

The thermodynamic relevance of the quantity ϕ has been well reported for a number of binary liquid alloys [36, 38, 43]. The expression of ϕ that incorporates both the entropic (via the number of self-associates, n) and the enthalpic contributions (via the interaction energy parameter, W) is given [42] as:

$$\phi = 1 - c_A c_B f(n, W) \quad (19)$$

Taking the last term of Eq. (3) with Eqs. (7), (17) and (19), one obtains the expression for viscosity in terms of the entropy and enthalpy as in [42]:

$$\frac{\Delta\eta}{\eta_o} = -c_A c_B f(n,W) \quad (20)$$

where $\Delta\eta = \eta - \eta_o$ is the deviation in η.

The factor f(n, W) is responsible for the characteristic behavior of viscosity for a given binary alloy. In the light of Conformal solution [42, 44, 45], another expression for viscosity is written in terms of the enthalpy of mixing, H_M as:

$$\frac{\Delta\eta}{\eta_o} = -\frac{H_M}{RT} \quad (21)$$

R is the universal gas constant.

2.3. Surface Properties: Surface Concentration and Surface Tension

The grand partition functions set up for the surface layer and that of the bulk provides a link between the bulk and the surface properties within the frame of the statistical mechanical approach through the concept of layered structure near the interface [46, 47]. This linkage connects the surface, c_i^S and bulk, c_i^b concentrations in terms of surface tension, σ via a pair of net equation:

$$\begin{aligned}\sigma &= \sigma_A + \frac{k_B T}{S}\ln\frac{c_A^s}{c_A^b} + \frac{k_B T}{S}\ln\frac{\gamma_A^s}{\gamma_A} \\ &= \sigma_B + \frac{k_B T}{S}\ln\frac{c_B^s}{c_B^b} + \frac{k_B T}{S}\ln\frac{\gamma_B^s}{\gamma_B}\end{aligned} \tag{22}$$

where σ_A and σ_B are the surface tensions of the components A and B, respectively. S is the mean atomic surface area of the alloy, calculated using the relation [46]:

$$S = \sum_i c_i S_i \quad (i = A, B) \quad and \quad S_i = 1.102\left(\frac{\Omega_i}{N_o}\right) \tag{23}$$

Ω_i is the atomic volume and N_o is the Avogadro's number. c_i^S and γ_i^S refer to the concentration and activity coefficient of the i^{th} component at the surface, respectively. γ_i and γ_i^S are related by:

$$\ln\gamma_i^s = p[\ln\gamma_i(c_i^s) + q\ln\gamma_i] \tag{24}$$

here p and q are the surface coordination fractions defined as the fractions of the total number of nearest neighbours of an atom in its own layer and that in the adjoining layer. As a consequence, p + 2q = 1. For a closed-packed structure the values of these parameters usually are taken as p = 0.5 and q = 0.25, respectively [48].

3. Results and Discussion

The thermodynamic data used for the modelling of the bulk thermodynamic properties of liquid Cr-Mo and Cr-Fe alloys at 1471 K and 1600 K, respectively, were taken from [14, 22]. The basic inputs for the computation of the bulk properties are the interaction energy parameter, W, its temperature dependence ∂W/∂T, and the number of self-associates, n, all listed in Table 1 for each of the two liquid alloys investigated. The values of these parameters (W, ∂W/∂T and n) were adjusted by the method of successive approximation to give the concentration dependence of activity, a_i, G_M/RT, H_M/RT, S_M/R and $S_{cc}(0)$ that reproduces fairly well the corresponding thermodynamic data as shown in Figs. 1 to 6. The interaction energy parameters for liquid Cr-Mo and Cr-Fe alloys, expressed in RT units, are W = 1.6200 and 0.7100, in that order, and remain invariant in all calculations.

Table 1. Energy parameters used for the bulk properties calculations

Alloy	T(K)	$\frac{W}{RT}$	n	$\frac{\partial W}{\partial T}$
Cr-Mo	1471	1.6200	0.7850	1.0850
Cr-Fe	1600	0.7100	0.6520	1.4593

3.1. Thermodynamic Properties: a_i, G_M, H_M and S_M

Figs. 1 and 2 show the plot of the calculated component activities of each liquid alloys studied compared with the respective experimental data. In Fig. 1, activity of Cr was compared at two different temperatures 1471 K [14] and 1873 K [22] for which experimental values exists in the literature. It can be noticed that there are fairly reasonable agreement between the calculated and experimental data especially below 0.7 atomic faction of Mo in Cr-Mo at 1471 K, while a_{Cr} in Cr-Mo has better agreement below 0.5atomic faction at 1471 K and also at $c_{Cr} > 0.5$ for a_{Cr} at 1873 K in Cr-Mo liquid alloys (Fig. 1). Above these concentrations, the calculated values show some form of disagreement with experimental data. Since activity is one of the thermodynamic functions that can be measured directly from experiment, the inconsistencies observed could suggest further assessment of thermodynamic activity data of Cr-Mo liquid alloys. On the other hand, Fig. 2 shows excellent agreement with experimental data of component activities of Cr and Fe in Cr-Fe liquid alloys at 1600 K, with the activity values very close to ideal behaviour for a_{Cr} and a_{Fe}, respectively, [1, 14].

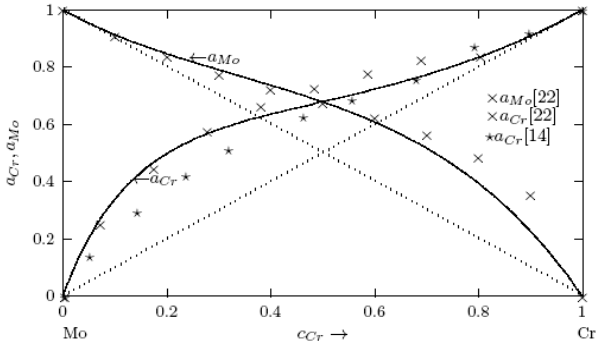

Figure 1. Concentration dependence of component activities a_{Cr} and a_{Mo} in Cr-Mo liquid alloys computed using Eqs. (11) and (12) at 1471 K, respectively. ⋆ ⋆ . . .and *x x*. . . are measured activity data at 1873 K and 1471 K, respectively. The solid lines denote calculated values. c_{Cr} is the bulk concentration of Cr in the alloy

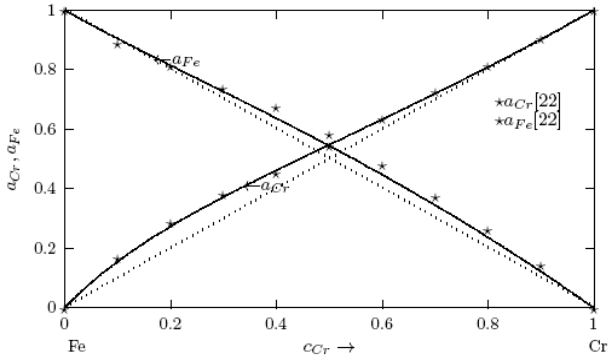

Figure 2. Concentration dependence of component activities a_{Cr} and a_{Fe} in Cr-Fe liquid alloys computed using Eqs. (11) and (12) at 1600 K, respectively. Symbol ⋆⋆. . . measured activity data at 1471 K. The solid lines denot calculated values. *cCr* is the bulk concentration of Cr in the alloy

The concentration dependence of G_M/RT computed using Eq. (2) for the two liquid alloys are presented in Fig. 3 with the respective experimental data, including the symmetry of the curves describing the G_M/RT vs. c_{cr} at the equiatomic composition. The degree of compound formation tendency in liquid alloys can be gauged by the normalized form of the Gibbs free energy of mixing of liquid phase at the equiatomic composition. The values of G_M/RT between 0 and -1 are characteristic for weakly interacting systems, those between -1 and -2 indicate systems with moderate interactions, while the values lower than -3 are typical of strongly interaction systems [38, 49, 50]. From Fig. 3, it is observed that the curves describing the G_M/RT show excellent agreement between calculated and experimental values across the whole concentration range with Cr-Mo and Cr-Fe liquid alloys exhibiting minimum G_M values of -0.3419 RT and -0.5773 RT at $c_{Cr} = 0.5$, respectively, indicating that the tendency of compound formation in the liquid phase of these systems is weak in nature. Also from Fig. 3, one can deduce that the degree of segregation in Cr-Mo with (G_M^{Min} = -0.3419 RT) is higher than in Cr-Fe with (G_M^{Min} = -0.5773 RT). The excellent agreement between the two sets of data also suggests that the choice of n and W used for the model calculations is quite reasonable.

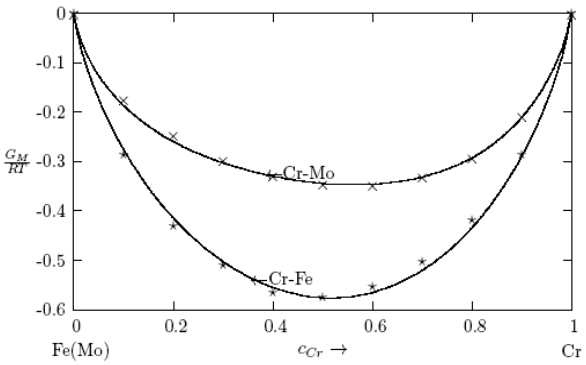

Figure 3. Concentration dependence of free energy of mixing, G_M/RT of Cr-Fe and Cr-Fe liquid alloys at 1471 K and 1600 K, respectively. The solid line denotes theoretical values, while times and stars denote experimental data [22] for Cr-Mo and Cr-Fe at respective temperatures. c_{Cr} is the bulk concentration of Cr in the alloy

The enthalpy of mixing, H_M and the entropy of mixing, S_M have been calculated from Eqs.(13) and (15), in that other, using the same interaction parameters given in Table 1 as used in computing a_i and G_M. The plots of H_M/RT and S_M/R versus c_{Cr} for the two Cr-based liquid alloys investigated at 1471 K and 1600 K are depicted respectively in Figs. 4 and 5, which show that like the experimental values [14], both H_M and S_M are positive at entire concentrations of Cr. There exists a reasonable agreement between calculated and experimental values.

The values of maxima in H_M/RT (Fig. 4) are observed around c_{Cr} = 0.46 with H_M/RT = 0.5965 and 0.4338 for Cr-Mo and Cr-Fe liquid alloys respectively, corresponding to stoichiometric concentration about the equiatomic composition. It is interesting to observe that the isotherms describing both the calculated and experimental values of the H_M/RT and S_M/R for the two liquid alloys are symmetric with respect to the equiatomic composition (typical of segregating alloys) [36]. The S_M/R shows maxima values of 0.9373 and 1.0042 at $c_{Cr} = 0.5$ for Cr-Mo and Cr-Fe liquid alloys, respectively (Fig. 5). We observed during the computation that if the interaction energy parameters are assumed to be temperature independent, (i.e. if $\partial W/\partial T = 0$), both H_M/RT and S_M/R so obtained were very inconsistent with experimental values. The theoretical analysis reveals that the interaction energy parameter, W is temperature dependent.

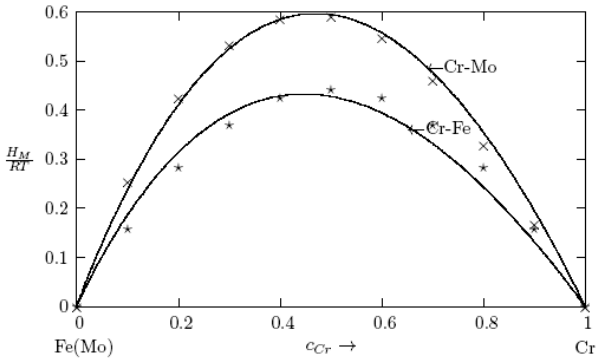

Figure 4. Concentration dependence of enthalpy of mixing, H_M/RT of Cr-Fe and Cr-Fe liquid alloys at 1471 K and 1600 K, respectively. The solid line denotes theoretical values, while times and stars denote experimental data [22] for Cr-Mo and Cr-Fe at respective temperatures. c_{Cr} is the bulk concentration of Cr in the alloy

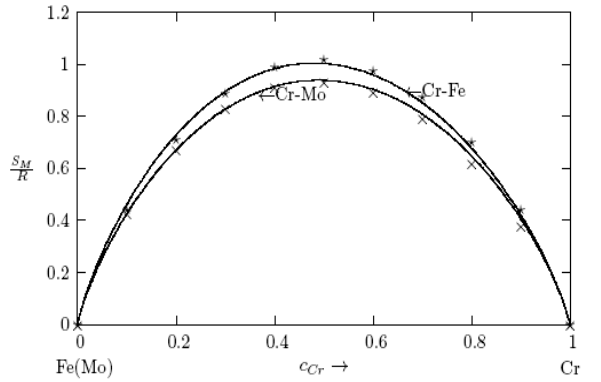

Figure 5. Concentration dependence of entropy of mixing, S_M/R of Cr-Fe and Cr-Fe liquid alloys at 1471 K and 1600 K, respectively. The solid line denotes theoretical values, while times and stars denote experimental data [22] for Cr-Mo and Cr-Fe at respective temperatures. c_{Cr} is the bulk concentration of Cr in the alloy

3.2. Microscopic Functions: $S_{cc}(0)$ and α_1

The concentration-concentration fluctuations in long-wavelength limits, $S_{cc}(0)$ has emerged as a very useful thermodynamic function to investigate the atomic order in a binary liquid alloy. The deviation of $S_{cc}(0)$ from the ideal values $S_{cc}^{id}(0) = c_A(1-c_A)$ (Eq. 8) can be used as a measure of the nature of atomic order and the stability of the mixture at a given composition. If at a given composition, $S_{cc}(0) > S_{cc}^{id}(0)$, there is a tendency of segregation. On the

contrary, $S_{cc}(0) < S_{cc}^{id}(0)$ refers to hetero-coordination. The theoretical values of $S_{cc}(0)$ are computed via Eq.(6) using the same interaction parameters used to compute G_M. The measured $S_{cc}(0)$ were determined from the experimental Gibbs free energy of mixing data taken from [14] when Eq.(5) is solved numerically. The results are shown in Fig. 6. From the figure, it is evident that the computed $S_{cc}(0) > S_{cc}^{id}(0)$ across the entire concentration range of Cr for both Cr-Mo and Cr-Fe liquid alloys at 1471 K and 1600 K, respectively. This suggests that both Cr-Mo and Cr-Fe are segregating liquid alloys. The degree of deviation observed around the equiatomic composition in Cr-Mo is about 62% higher than that of Cr-Fe. That is to say that homo-coordination of atoms (preference for like atoms to be paired as nearest-neighbours) exists in these molten alloy systems, which is consistent with positive values of the interaction energy parameter, W. Also from Table 1, it can be observed that when n and W are less than 1 for Cr-Fe alloys, the $S_{cc}(0)$ exhibits symmetrical behaviour at equiatomic composition with $c_{Cr} = 1/2$, whereas, Cr-Mo liquid alloys with $n < 1$ and $W > 1$, exhibits asymmetry and positive deviation in $S_{cc}(0)$ as expected as a function of both n and W. However, the positive deviation observed in $S_{cc}(0)$ behaviour for Cr-Fe liquid alloys at 1600 K in this work contrast sharply with the results of Novakovic and Brillo [1] who used the quasi-chemical approximation for regular alloys and reported that Cr-Fe alloys exhibited negative deviation with $S_{cc}(0) < S_{cc}^{id}(0)$ at 1873 K.

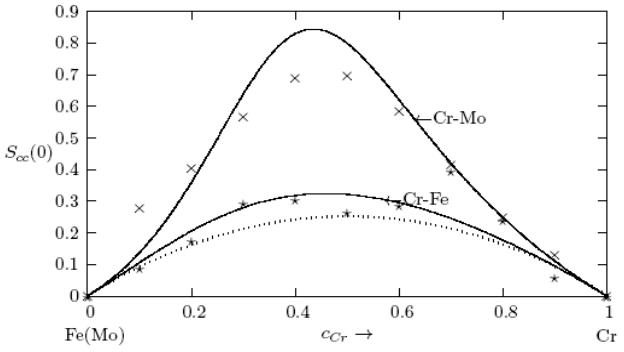

Figure 6. Concentration-concentration fluctuations at long wavelength limits, $S_{cc}(0)$ as a function of concentration for Cr-Mo and Cr-Fe liquid alloys at 1471 K and 1600 K, respectively. The solid line denotes theoretical values, while times and stars denote experimental data [22] for Cr-Mo and Cr-Fe at respective temperatures. The dots denote the ideal values of $S_{cc}(0)$. c_{Cr} is the bulk concentration of Cr in the alloy

In order to gain qualitative insight into the nature of arrangement of atoms, the Warren-Cowley short range order parameter, α1, was also computed for both liquid alloys studied. This parameter (α_1) can be evaluated theoretically using the knowledge of $S_{cc}(0)$ through Eq.(9). At equiatomic composition, one has $-1 \leq \alpha_1 \leq +1$. The minimum value of $\alpha_1 = -1$ implies complete ordering, $\alpha_1 = +1$ corresponds to segregation leading to the phase separation and $\alpha_1 = 0$ implies a random distribution of atoms. It is found from Fig. 7 that α_1 is positive at all concentrations of Cr in Cr-Mo and Cr-Fe liquid alloys which is indicative of segregation or phase separation as evident from $S_{cc}(0)$. In the present work, the value of α_1 has been computed with the coordination number, z = 10, as shown in Fig. 7. From the figure, the asymmetry in α_1 is distinctly visible at about $c_{Cr} = 0.4$. This further confirms earlier assertion that both Cr-Mo and Cr-Fe liquid alloys are segregating systems of like atoms (i.e. Cr-Cr, Mo-Mo or Fe-Fe) pairing as nearest-neighbours.

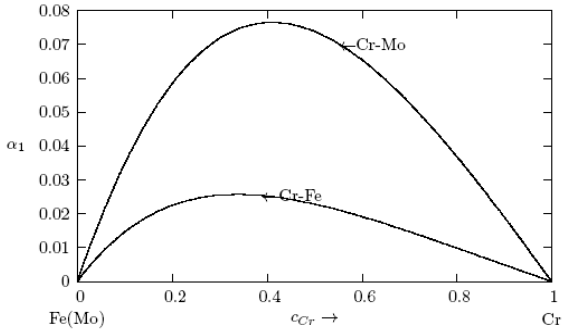

Figure 7. Warren-Coyley Short-range order parameter, (α_1), computed using Eq. (9) versus concentration for Cr-Mo and Cr-Fe liqud alloys at 1471 K and 1600 K, respectively. c_{Cr} is the bulk concentration of Cr in the alloys

3.3. Diffusion and Viscosity

The calculated values of $S_{cc}(0)$ are used in Eq.(16) to assess the ratio of the mutual and self-diffusion coefficients, D_M/D_{id}. The values of D_M/D_{id} are found to be less than 1 across the concentration range as presented in Fig. 8. This also indicates that the segregating feature of Cr-Mo and Cr-Fe liquid alloy as observed in $S_{cc}(0)$ and α_1. Since D_M/D_{id} sharply reduced to very small values in the region around $c_{Cr} \approx 0.41$ and 0.34 with distinct asymmetric features, where Cr-Mo and Cr-Fe liquid alloys have their minima values, respectively. The phase separating tendency in Cr-Mo and Cr-Fe liquid alloys at 1471 K and 1600 K is maximum at the intermediate composition.

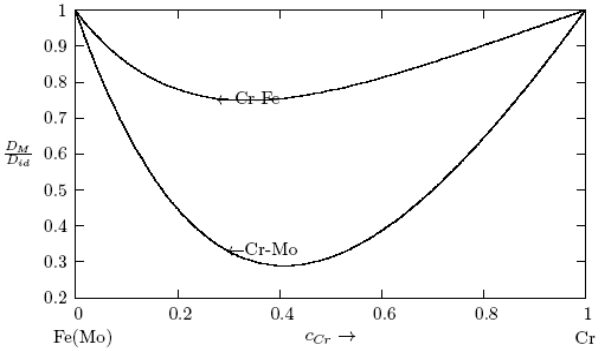

Figure 8. Diffusion coefficients, D_M/D_{id}, computed using Eq.(16) versus concentration for Cr-Mo and Cr-Fe liquid alloys at 1471 K and 1600 K, respectively. c_{Cr} is the bulk concentration in the alloys

Owing to chemical reactivity and affinity for oxygen by liquid metallic elements at elevated temperatures, experimental determination of viscosity data is usually very difficult [39]. This accounts for why a large missing gap exists between different sets of experimental data or a nearly

complete lack of viscosity data for many liquid alloys in literature. To overcome this challenges, many theoretical models have been proposed for estimating viscosity [42-43, 51-56], but none of the existing models is universally applicable to estimate viscosity data for a large class of liquid alloy systems. In this work, the expressions of viscosity due to Singh and Sommer [42] through Eqs. (20) and (21) have been used to model the viscosity of each liquid alloy. The negative values of experimental enthalpy of mixing calculated using Eq. (21) for Cr-Mo and Cr-Fe liquid alloys are the corresponding experimental values of viscosity for the alloys.

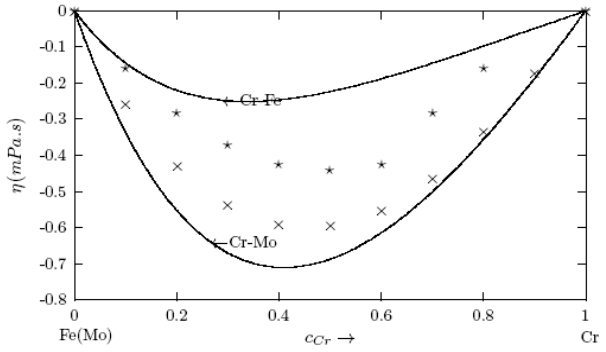

Figure 9. Concentration dependence of viscosity, η for Cr-Mo and Cr-Fe liquid alloys calculated using Eq. (20) at 1471 K and 1600 K, respectively. The solid line denotes theoretical values, while times and stars denote $-H_M/RT$ used as experimental data [22] via Eq. (21) for Cr-Mo and Cr-Fe liquid alloys at respective temperatures

To the best of authors' knowledge, the viscosity η of Cr-Mo liquid alloys has not yet experimentally been determined, while very old scatter data exists for Cr-Fe liquid alloys in literature [1, 57]. Fig. 9 shows the plot of the concentration dependence of viscosity for each liquid alloy at respective investigated temperatures. From the figure, it is seen that both the calculated and experimental viscosity isotherms for each liquid alloys show the same trend of negative deviation from ideality with asymmetric behaviour as observed in α_1 and D_M/D_{id}. As a rule, the compound forming systems are apt to exhibit maximum (due to positive deviations) in their isothermal viscosity [38, 46] in those composition ranges where intermetallic compounds are formed in the solid state. One would therefore expect for segregating alloys like Cr-Mo and Cr-Fe with positive H_M, to exhibit negative deviations of isothermal viscosity [36, 38, 58] as seen in Fig. 9 with positive values of W as well. The correlation between the calculated and experimental viscosity data shows a better agreement in Cr-Mo alloys than that of Cr-Fe liquid alloys.

3.4. Surface Properties

Using the parameters given in Tables 1 and 2 as input and the required activities as obtained from the relevant expressions in the model, the surface concentration of Cr has been computed by solving Eq. (22) simultaneously. These surface concentrations were used to evaluate the surface tension as a function of bulk concentration, c*i* (*i* = Cr) for Cr-Mo and Cr-Fe liquid alloy at the working temperatures.

Table 2. Essential parameters used for the surface properties calculation for Cr-Mo and Co-Fe at respective temperatures

Atom	$\sigma(Nm^{-1})$[56]	$\frac{d\sigma}{dT}(mNm^{-1}K^{-1})$[56]
Cr at 1471 K	1.9262	-0.3200
Mo at 1471 K	2.6914	-0.3100
Cr at 1600 K	1.8850	-0.3200
Fe at 1600 K	1.9940	-0.4900

The relations between the temperature dependence of surface tension and atomic volume have been used to get the atomic volumes required for the computation of surface concentration and surface tension, and these are given as [35, 56]:

$$\sigma_i = \sigma_{im} + (T - T_m)\frac{\partial \sigma_i}{\partial T} \tag{25}$$

and

$$\Omega_i = \Omega_{im}[1 + \theta(T - T_m)] \tag{26}$$

where θ is the thermal coefficient of expansion, Ω_{im}, σ_{im} are the atomic volume and surface tension of the alloy components at their melting temperature T_m and T is the working temperature in Kelvins. The values of $\partial\sigma i/\partial T$ and θ for the pure components of the alloys Cr, Mo and Fe were obtained from [56]. S and Si for each atomic species of the alloy systems were computed using Eq. (23).

Lack of sufficient experimental data on surface properties for the two liquid alloys at the working temperatures justify the interest that can be given to the theoretical investigations. In particular, the concentration dependent data of surface tension (σ) for segregating liquid alloys are scarce [36]. Fig. 10 shows the results of the computed values of surface concentration of Cr as a function of bulk concentration for the two liquid alloys. The structural analysis shows that as bulk concentration of Cr in Cr-Mo liquid alloys increases, the surface concentration c_{Cr}^{s} remain constant at about 0.11% up till about 40% bulk concentration when it begins to rise sightly with increasing bulk concentration. At 96.5% and 98.9% bulk concentrations, the surface concentrations are 17.56% and 53.42%, respectively. This is an indication that in the alloy there are more atoms of component with bigger atomic size (i.e. Mo-atoms with atomic size of 9.38 [59], compared to Cr with 7.23 [59]) at the surface. Hence, at the surface of Cr-Mo, more Mo-atoms segregate at the surface in preference to Cr-atoms up to around 98.9% bulk concentration.

On the other hand, the calculated values of surface concentration, c_{Cr}^{S}, in Cr-Fe liquid alloys (Fig. 10) suggest the segregation of Cr-atoms to the surface as the bulk concentration increases. The rate at which Cr- atoms segregates to the surface is nearly proportional to the rate at which it segregates to the bulk surface with the surface isotherm curve for Cr- Fe liquid alloys almost close to ideal mixture behaviour. This implies that Cr-atoms with lower

value of surface tension with respect to Fe-atoms tend to segregate to the surface, while the Fe-atoms with higher surface tension value prefer to remain in the bulk in the molten alloy. A closer look at the surface isotherm curve also reveals that Cr-Fe liquid alloy exhibits a slight positive to negative deviations with respect to the ideality c_{id}^{S}. It may be point out here that when there is a significant difference in surface tension values between the solvent and solute, the mixing shows strong segregation of the component with lower surface tension at the surface and the other in the bulk [6, 60].

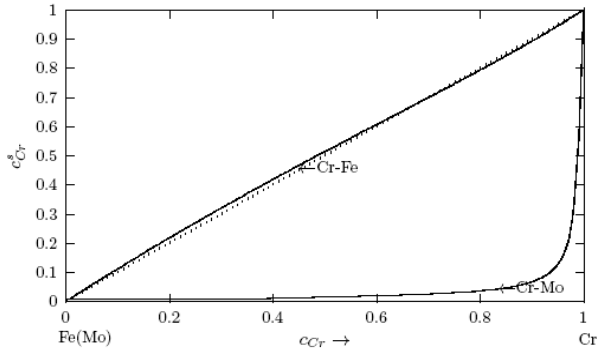

Figure 10. Computed values of the surface concentrations of Cr in Cr-Mo and Cr-Fe liquid alloys at 1471 K and 1600 K, respectively. The curves were computed via Eq. (22). The dots denote the ideal values of the surface concentration, c_{id}^{S} computed from: $c_{id}^{S} = c^{b}$. c_{Cr} is the bulk concentration of Cr in the alloys

Comparison of the two surface isotherm curves describing the surface segregation reveals that the rate at which Cr-atoms segregate at the surface of Cr-Fe liquid alloys is more than the rate at which Cr-atoms segregate at the surface in Cr-Mo liquid alloys for all bulk concentrations. For instance, at the same bulk concentration when c_{Cr} is equal to 40%, the surface is enriched with about 0.11% of Cr-atoms in Cr-Mo whereas about 42% of Cr- atoms segregate at the surface of Cr-Fe alloys. The enrichment of the surface of Cr-Fe alloys with Cr-atoms could be due to the fact that there exists a higher tendency for unlike atoms to pair as nearest neighbours in Cr-Fe alloys, than in Cr-Mo alloys which shows a higher degree of segregation as earlier observed for $S_{cc}(0)$ and α_1. On the contrary, with very comparable values of the surface tension of the metals as noticed in Cr-Fe liquid alloy, the surface concentrations do not differ much from the bulk compositions.

The surface tensions of the liquid alloys were computed by putting the surface concentration (c_i^s) values, W, surface coordination fractions (p and q), mean atomic surface area (S) and surface tension data of pure components (σ_A and σ_B) into Eq. (22). Surface tension data of pure Cr, Mo and Fe metals were taken from [56]. The surface tension isotherms of Cr-Mo and Cr-Fe liquid alloys exhibit negative deviations from corresponding ideal mixture isotherms as shown in Figs. 11 and 12, respectively.

The result shows that surface tension of Cr-Mo liquid alloy increases with increase in the bulk concentration of metal with lower surface tension (i.e. Cr-atoms) (Fig. 11). Whereas, the surface tension of Cr-Fe liquid alloy initially decreases with increasing bulk concentration to about 70% bulk concentration and then rises as seen in Fig. 12. The negative deviation between calculated surface tension isotherms of both systems and ideal values of the surface tensions substantiates earlier claim that the two liquid alloys are segregating systems. This submission remains consistent with the positive deviations of their bulk properties from the Raoult's law [60, 61]. However, due to lack of experimental data at the investigation temperatures, it was impossible to compare the calculated surface tension values with experimental values.

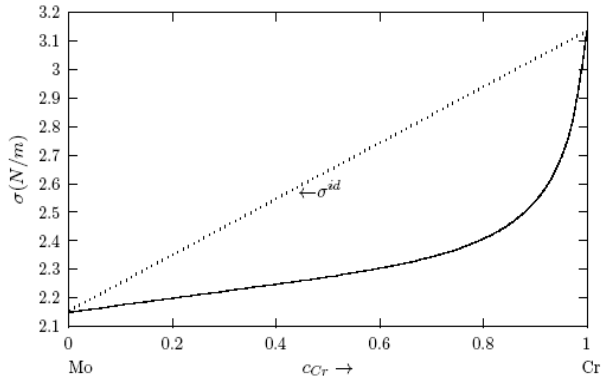

Figure 11. Computed values of the surface tension, σ for Cr-Mo liquid alloys at 1471 K, computed via Eq. (22). The dots labelled σ^{id} denote the ideal values of the surface tension obtained from the relation: $\sigma^{id} = \sigma_A c_A + \sigma_B c_B$. c_{Cr} is the bulk concentration of Cr in the alloy

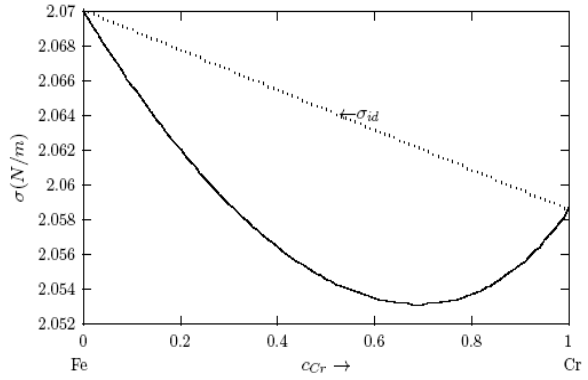

Figure 12. Computed values of the surface tension, σ for Cr-Fe liquid alloys at 1600 K, computed via Eq.(22). The dots labelled σ^{id} denote the ideal values of the surface tension obtained from the relation: $\sigma^{id} = \sigma_A c_A + \sigma_B c_B$. c_{Cr} is the bulk concentration of Cr in the alloy

4. Concluding Remarks

The theoretical study shows positive deviation in the mixing properties from the ideal mixture behaviour indicating segregation in Cr-Mo and Cr-Fe liquid alloys. The degree of segregation is more in Cr-Mo alloy at 1471 K than in Cr-Fe system at 1600 K as evident in their investigated bulk properties. It was pointed out that when there is a

significant difference in surface tension values between the solvent and solute, the mixing shows strong segregation of the component with lower surface tension at the surface and the other in the bulk. The surface tension study also reveals that addition of Cr-atoms leads to increase in surface tension of Cr-Mo and Cr-Fe liquid alloys across bulk concentration expect for bulk concentration < 70% in Cr-Fe, where σ decreases with increasing bulk concentrations. The decrease in σ of Cr- Fe alloys for bulk concentration in the range of $0 \leq c_{Cr} \leq< 0.7$ indicates that more atoms of components with bigger atomic size (i.e. Cr-atoms) segregates at the surface in preference to Fe-atoms. In addition, the rates at which Cr-atoms segregate at the surface of Cr-Fe liquid alloys is more than the rate at which Cr-atoms segregate at the surface in Cr-Mo liquid alloys for all bulk concentrations. This segregation of the components may result from the differences in atomic size, surface tension and electron configuration between the components of an alloy. The possible roles of the entropic and enthalpic effects on the phase-segregation observed in the two liquid alloys have been explained in terms of the bulk and surface properties.

REFERENCES

[1] R. Novakovic and J. Brillo, J. Molecul. liq., 200 (2014) 153-159.

[2] C. Costa, S. Delsante, G. Borzone, D. Zivkovic, R. Novakovic, J. Chem. Thermodyn., 69 (2014) 73-84

[3] Z. Grzesik, Z. Jurasz, K. Adamaszek, S. Mrowec, High Temp. Mater, Process, 31(6) (2012) 775-779.

[4] C. Fazio, A. Alamo, A. Almazouzi, S. De Grandis, D. Gomez-Briceno, J. Henry, L. Malerba, M. Rieth, J. Nucl. Mater. 392 (2009) 316-323

[5] B. Zheng, Y. Zhou, J.E. Smugerresky, E.J. Lavernia, Metall. Mater. Trans. A 40 (2009) 1235-1245.

[6] R. Novakovic, J. Phys.: Condens. Matter 23 (2011) 235107 (8pp).

[7] P. H. Mayrhofer, H. Willmann, and A. E. Reiter, Surf. and Coatings Techn., 202 (2008) 4935-4938.

[8] P. H. Mayrhofer et al., Progress in Materials Science 51 (2006) 1032- 1114.

[9] P. Hones, R. Sanjins, and F. Lvy, Thin Solid Films 332 (1998) 240-246.

[10] B. Gu et al., Surf. and Coatings Technn. 202 (2008) 2189-2193.

[11] L. Zhou, H. David, and H. M. Paul, J. Phys. D: Appl. Phys. 46 (2013) 365301.

[12] A. Magnli, Acta Crystallographica 6 (1953) 495.

[13] G. Gassner et al., Surf. and Coatings Techn. 201 (2006) 3335-3341.

[14] K.T. Jacob, B.V. Kumar, Z. Metallkd. 77 (1986) 207-211.

[15] M. Laffitte, O. Kubaschewski, Trans. Faraday Soc. 57 (1961) 932.

[16] O. Kubaschewski, T.G. Chart, J. Inst. Met. 93 (1965) 329-338.

[17] D.S. Dickson, J.R. Myers, M.J. Pool, R.K. Saxer, Trans. Metall. AIME 245 (1969) 175-177

[18] S. Hertzman, B. Sundman, Calphad 6 (1982) 67-80.

[19] J.O. Andersson, TRITA- MAC-0207, KTH, 1982.

[20] Y.Y. Chuang, J.C. Lin, Y.A. Chang, Calphad 11 (1987) 57-72.

[21] J.C. Lin, Y.Y. Chuang, K.C. Hsieh, Y.A. Chang, Calphad 11 (1987) 73-81.

[22] R. Hultgren, P.D. Desai, D.T. Hawkins, M. Gleiser, K.K. Kelly, Selected Values of the Thermodynamic Properties of binary Alloys, American Society of Metals, Ohio, 1973.

[23] J.O. Andersson, B. Sundman, Calphad 11 (1987) 83-92.

[24] B.-J. Lee, CALPHAD 17 (1993) 251-268.

[25] J. Vretl, J. Houserov, M. ob, J. Min. Metall. Sect. B 38 (2002) 205-211.

[26] J.-C. Lin, Y.-Y. Chuang, K.-C. Hsieh, Y.A. Chang, Calphad 11 (1987) 73-81

[27] W. Xiong, M. Selleby, Q. Chen, J. Odqvist, Y. Du, Crit. Rev. Solid State Mater. Sci. 35 (2010) 125-152.

[28] W. Xiong, P. Hedstrom, M. Selleby, J. Odqvist, M. Thuvander, Q.Chen, Calphad 35 (2011) 355-366.

[29] R.M. Fisher, E.J. Dulis, K.G. Carroll, Trans. Am. Inst. Min. Metall. Pet. Eng. 197 (1953) 690-695.

[30] C.X. Quintela, B. Rodrguez-Gonzlez, and F. Rivadulla, Appl. Phys. Lett. 104 (2014) 022103-5.

[31] S. Swaminathan, K.T. Jacob, Bull. Alloy Phase Diagrams 10 (1989) 329-331.

[32] J.P. Neumann, Bull. Alloy Phase Diagrams 10 (1989) 524-524.

[33] K. Mills and Y.C. Su, Int. Mater. Rev., 51(6) (2006) 329-351.

[34] L. Pauling, Nature of the Chemical Bonding, Cornell University Press, Ithaca, NY. 1960.

[35] T. Iida, and R.I.L. Guthrie, The Physical Properties of Liquid Metals, Clarendon Press, Oxford, 1993.

[36] R.N. Singh, F. Sommer, Rep. Prog. Phys. 60 (1997) 57-150.

[37] Y.A. Odusote, L.A. Hussain, O.E. Awe, J. Non-Cryst. Solids 353 (2007) 1167-1171.

[38] R.N. Singh, N.H. March, in: J.H. Westbrook, R.L. Fleischer (Eds.), Intermetallic Compounds, Principles and Practice, Vol. 1, Wiley, New York. 1995, p.661-686.

[39] R. Novakovic, M.L. Muolo, and A. Passerone, Surf. Sci., 549 (2004) 281-293.

[40] R.N. Singh and F. Sommer, Z. fur Metallk. 83(7) (1992) 533-540.

[41] J.M. Cowley, Phys. Rev. 77 (1950) 669-675.

[42] R.N. Singh and F. Sommer, Phys. Chem. Liq., 36 (1998) 17-28.

[43] S.M. Osman, R.N. Singh, Phys. Rev. E. 51 (1995) 332.

[44] R.N. Singh, F. Sommer, J. Phys. Condens. Mat. 4 (1992) 5345-5358.

[45] R.N. Singh, F. Sommer, Z. Metallkd. 83 (1992) 533-540.

[46] L.C. Prasad, R.N. Singh, V.N. Singh and G.P. Singh, J. Phys. Chem. B, 102 (1998) 921-926.

[47] L.C. Prasad, R.N. Singh and G.P. Singh, Phys. Chem. Liq., 27(3) (1994) 179-185.

[48] E.A. Guggehheim, Mixtures, Oxford University Press, London, 1952.

[49] R. N. Singh, Can. J. Phys. 65 (1987) 309-325.

[50] I. Egry, E. Ricci, R. Novakovic, S. Ozawa, Adv. Colloid Interface Sci., 159 (2010) 198-212.

[51] E. A. Moelwyn-Hughes, Physical chemistry, Pergamon Press, Oxford, 1961, p19.

[52] J. Brillo, R. Brooks, I. Egry, P. Quested., Int. J. Mat. Res. (formerly Z. Metallkd.) 98 (2007) 6.

[53] I. Budai, M. Z. Benk o, G. Kaptay, Materials Science Forum Vol. 473- 474 (2005) 309.

[54] I. Budai, M. Z. Benk o, G. Kaptay, Materials Science Forum Vol. 537- 538 (2007) 489.

[55] T. Iida, and R. I. L. Guthrie,, The Physical Properties of Liquid Metals, Clarendon Press, Oxford, 1993.

[56] Smithell's Metals Reference Book, in: W.F. Gale, T.C. Totemeir (Eds.), 8th Edition, Elsevier Butterworth-Heinemann, Oxford, 2004.

[57] J. Brillo, I. Egry, T. Matsushita, Z. Metallkd. 97 (2006) 28.

[58] Y.A. Odusote, J. Non-crystal. Solids, 402 (2014) 96-100.

[59] C.N. Singman, J. Chem. Education, 61(2) (1984) 137-142.

[60] R. Novakovic, T. Tanaka, M.L. Muolo, J. Lee, and A. Passerone, Surf. Sci., 591 (2005) 56-69.

[61] T. Tanaka, K. Hack, S. Hara, Mater. Research Sci. Bull.(1999) 45.